

POWER MODELING OF THE XRL HEXAPEDAL ROBOT AND ITS APPLICATION TO ENERGY EFFICIENT MOTION PLANNING

Camilo Ordonez*, Nikhil Gupta, Emmanuel G. Collins, Jr., Jonathan E. Clark
*Mechanical Engineering, Florida A&M University-Florida State University,
Tallahassee, FL 32310, USA*
**E-mail: camilor@eng.fsu.edu*

Aaron M. Johnson
*Electrical and Systems Engineering, University of Pennsylvania,
Philadelphia, PA 19104, USA*

Analysis of the power consumption for walking and running robots is particularly important for trajectory planning tasks as it enables motion plans that minimize energy consumption and do not violate power limitations of the robot actuators. This paper builds upon previous work on wheeled skid-steered robots, and for curvilinear motion of the XRL hexapedal robot, presents models of the inner and outer side torques and power requirements. In addition, the applicability of the power model to energy efficient motion planning is illustrated for a walking gait on a vinyl surface.

Keywords: skid-steering; turning for legged robots.

1. Introduction

The ability to predict power demands is an important capability for energetically constrained robot motion planning. In particular, the development of robot power models aids in four important areas of robot motion planning:

- (1) Motion planning with actuator power limitations,
- (2) Energy efficient path/trajectory planning,
- (3) Task completion prediction based on available energy,
- (4) Planning for refueling or recharging.

Recent work on skid-steered vehicles has led to the formulation of analytic dynamic and power models that rely on the terramechanics of wheel-terrain interactions, in particular, models based on the exponential relationship between shear stress and shear displacement at the contact

patch. These models have been verified on flat and rigid surfaces for steady state turning maneuvers.¹ Reduced order models that relax some of the assumptions of the terramechanics models have also been derived for skid-steered vehicles.²

While the ground contact patterns for legged robots and in particular the RHex-like robots considered here,³ are characterized by discrete rather than continuous contact, some work has been done to experimentally develop kinematic models of these systems.³ There has been some related work focused on reducing power (or specific resistance) of these systems, but not specifically on modeling the power.⁴

The present work is motivated by the hypothesis that for certain regimes of operation (i.e., certain gait parameters), legged robots from the RHex family behave in a similar fashion to skid-steered robots while in general curvilinear motion. The remainder of the paper is organized as follows: Section 2 presents a short description of the experimental platform and its approximated kinematics. Section 3 details the developed torque and power models. Section 4 presents an illustrative example of the application of the developed model on energy efficient motion planning. Finally, Section 5 provides concluding remarks and directions for future work.

2. Robotic Platform and Approximated Kinematics

The XRL (X-RHex Light) experimental platform^{5,6} employed in this research and shown in Fig. 1 is a very versatile, slightly lighter version of the X-RHex robot, capable of performing diverse gaits, including walking, jogging, running and pronking. The robot has 6 compliant C-shaped legs independently actuated by 50 Watt Brushless Maxon motors with a gear ratio of 18:1.



Fig. 1. XRL Robot Utilized as the Experimental Platform for this Work.

For this paper we will consider an alternating tripod gait for the XRL locomotion. Referring to Fig. 2, the alternating tripods correspond to a left tripod formed by legs 1,3, and 5 and a right tripod formed by legs 2,4, and 6.

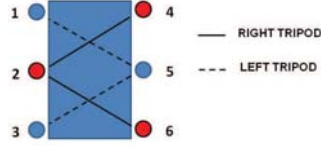


Fig. 2. Left and Right Tripods for XRL.

Each of the tripods follows at the low level a desired trajectory generated by a Buehler clock,³ which characterizes the gait by four parameters: the frequency f [Hz], nominal duty factor \overline{d}_f , nominal leg offset $\overline{\phi}_0$ [rad] and the nominal leg sweep angle $\overline{\phi}_s$ [rad]. These parameters are grouped into the control vector $u = [f, \overline{d}_f, \overline{\phi}_0, \overline{\phi}_s]^T$, where the frequency and duty factor are expressed in terms of the cycle t_c and stance t_s times by ($f = \frac{1}{t_c}$ and $\overline{d}_f = \frac{t_s}{t_c}$).

In order to turn while in motion, perturbations on the gait parameters for the inner (1,2,3) and outer (4,5,6) legs are introduced (hereafter we assume left hand turns). These perturbations are functions of a turn gain t_g and some extra constants (α, β, γ). The perturbed gait parameters for the inner legs are expressed by:

$$\phi_o^i = \overline{\phi}_o - t_g \alpha, \quad (1)$$

$$\phi_s^i = \overline{\phi}_s - t_g \beta, \quad (2)$$

$$d_f^i = \overline{d}_f - t_g \gamma. \quad (3)$$

The outer legs parameters ϕ_o^o , ϕ_s^o , and d_f^o are computed similarly but with opposite signs for the perturbations. For all experiments performed in this work, $\alpha = 0.05$, $\beta = 0.7$, and $\gamma = 0.0$. The robot kinematics were derived by conducting experiments for turning gains in $\{0.0, 0.04, 0.1, 0.2, 0.4, 0.5, 0.6\}$ and frequencies in $\{0.5, 0.6, 0.7, 0.8, 0.9, 1.0, 1.1\}$ Hz using a walking gait parameterized by $u = [f, t_g, 0.65, -0.314, 0.785]^T$. Robot forward velocity and turn radius were measured by tracking with a high-speed digital camera (Casio Exilim EX-F1) a set of LEDs mounted on the robot. Figs. 3 and 4 summarize the approximated kinematics for the walking gait on a vinyl surface. In particular, the robot forward velocity v [m/s] and the robot turn radius ρ [m] are approximated by:

$$v = 0.16f, \quad (4)$$

$$\rho = 13.92e^{-5.78t_g} + 0.764. \quad (5)$$

It is important to note that, as can be seen from Figs. 3 and 4, no clear dependence of the velocity on the turn gain and of the turn radius on the frequency was observed and that is the reason why Eqs. 4, and 5 depend

only on one variable. To generate these models, the experimental data set was split using 80% of the data for model fitting and 20% for validation, which yielded average prediction errors of 4.1% for the forward velocity and 17.7% for the turn radius.

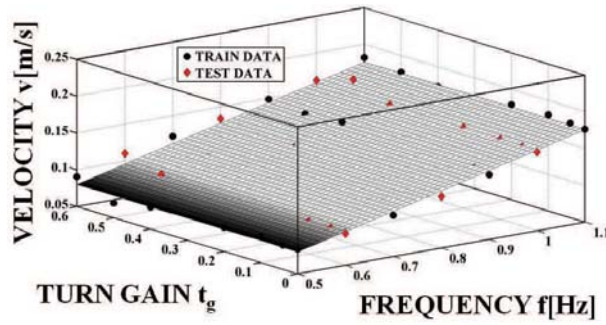


Fig. 3. XRL Kinematics (forward velocity).

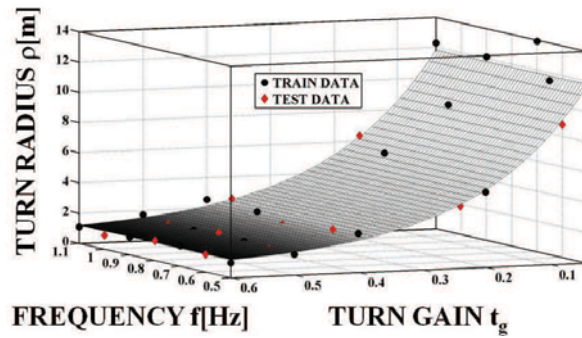


Fig. 4. XRL Kinematics (turn radius).

3. Torque and Power Model

During the experiments described in Section 2, motor torques τ for each leg were monitored. Then, the average torques per cycle for the inner and outer legs were estimated using:

$$\bar{\tau}_i = \overline{\tau_1(t) + \tau_2(t) + \tau_3(t)}, \quad t \in [0, tc], \quad (6)$$

$$\bar{\tau}_o = \overline{\tau_4(t) + \tau_5(t) + \tau_6(t)}, \quad t \in [0, tc], \quad (7)$$

where \bar{x} is the average of x . Fig. 5 shows that the torques follow clear exponential trends as a function of turn radius, which is qualitatively similar to the torque vs turn radius curves observed for skid-steered robots.^{1,2} Notice that as the turn radius increases, the torques tend to a small value

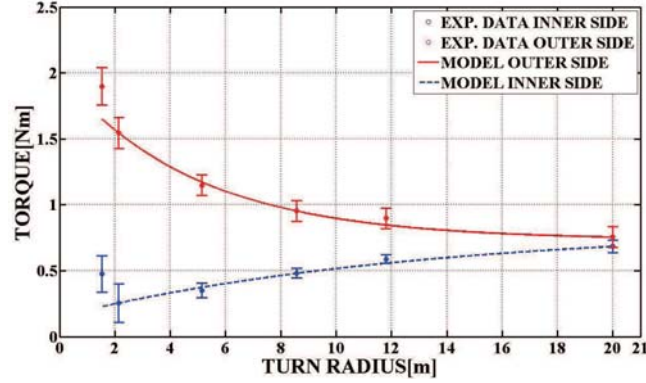


Fig. 5. XRL: Inner and Outer Side Torques as a Function of Turn Radius.

which is associated with the rolling resistance (error bars represent torque standard deviation for the different speeds).

The validation turn radii ρ are in the set $\{5.14, 11.81\}m$. For these ρ , the fitted models yield average prediction errors of 3.81% for the outer side and 6.04% for the inner side. For turn radii of less than 2.14m, the model does not capture the behavior of the inner side torque, perhaps due to the fact that for these sharper turns roll motion is increased, making the gait less stable and modifying the steering dynamics significantly.

Power for the inner and outer sides was computed by adding the mechanical power and the electrical losses as follows:

$$P_i = \overline{\sum_{j=1}^3 (|\tau_j(t)w_j(t)| + I_j^2(t)R)}, \quad t \in [0, tc], \quad (8)$$

$$P_o = \overline{\sum_{j=4}^6 (|\tau_j(t)w_j(t)| + I_j^2(t)R)}, \quad t \in [0, tc], \quad (9)$$

where w_j is the angular velocity of leg j , I_j is the current through the motor corresponding to leg j and R is the phase to phase electrical resistance of each of the six motors. Motivated by insight gained from power modeling of skid-steered robots,² we look for a model of similar shape where power is related to velocity and turn radius by

$$P = a(\rho)v + b(\rho), \quad (10)$$

where a and b are coefficients dependent on the turn radius. Experimental curves shown in Figs. 6 and 7 relating power and speed for different turn radii were obtained for both the inner and outer robot sides. Straight lines were then fitted to data corresponding to each turn radius and their intercepts and slopes were used to estimate the power model parameters a and b for both robot sides. These parameters are summarized in Table 1. The power model was then evaluated at the test speeds v in the

set $\{0.096, 0.128, 0.16\}$ m/s, yielding average errors over all turn radii of 8.69% and 9.19% for the outer and inner side respectively.

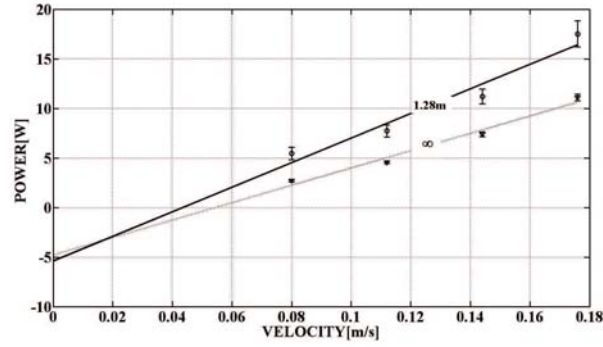


Fig. 6. Inner Side Power Curves (only two turn radii (1.28m and ∞) are shown for ease of visualization).

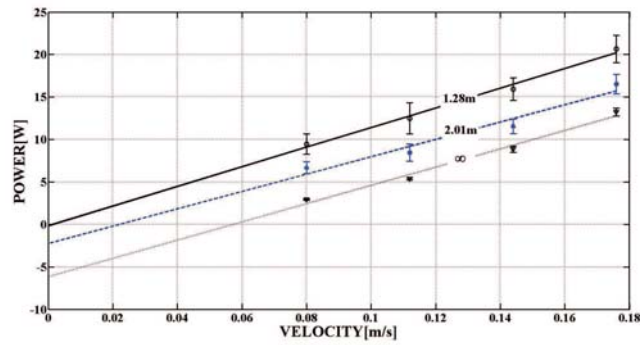


Fig. 7. Outer Side Power Curves (only three turn radii are shown for ease of visualization).

Table 1. Power Model Parameters.

INNER SIDE		OUTER SIDE	
$a_i(\rho)$	$b_i(\rho)$	$a_o(\rho)$	$b_o(\rho)$
$240.6e^{-1.26\rho} + 88.82$	$-1.40e^{-0.07\rho} - 4.35$	106.9	$9.21e^{-0.34\rho} - 6.12$

4. Application of the Proposed Model To Energy Efficient Motion Planning

Using the power models developed in Section 3, it is possible to generate the power surface illustrated in Fig. 8, which combines the power of both robot sides. This power surface was then integrated with Sampling-Based Model

Predictive Optimization (SBMPO), which is a motion planning algorithm capable of planning efficiently with dynamic models.⁷ The outcome of this integration is the simulation result shown in Fig. 9, which compares paths obtained by optimizing a distance cost function and an energy cost function. Notice that energy efficient motion planning saved 33.5% in energy with only a 13.1% increase in distance traveled.

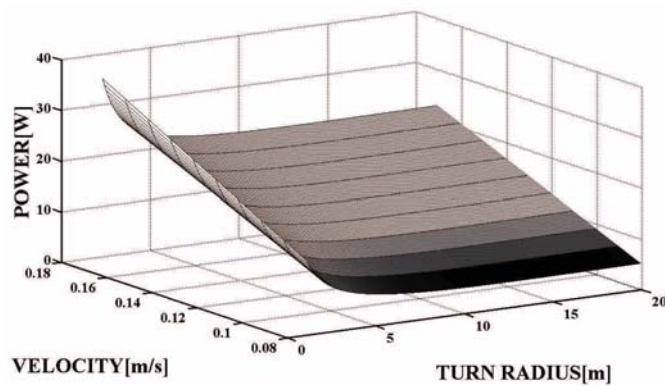


Fig. 8. XRL Power Surface.

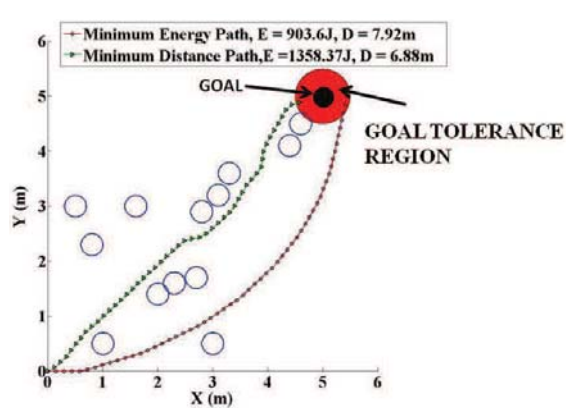


Fig. 9. Minimum Energy Vs Minimum Distance Paths.

5. Discussion and Future Work

Preliminary experimental results for a walking gait show significant similarities in the torque and power vs turn radius trends for the XRL and skid-steered wheeled vehicles. The observed similarities, suggest that at

least to some extent the frictional forces involved in the curvilinear motion of both platforms share some commonalities and should be exploited in the future to obtain an analytical model of the dynamics of turning for RHex-like robots.

In addition, initial path planning results using the obtained power model for a walking gait show that paths obtained using energy optimization tend to be smoother than the paths obtained using distance optimization since the power curves show that more power is needed for turns with small radius. Future work will involve the verification of these observations for different gaits and the experimental validation of the energy estimates obtained using SBMPO.

Acknowledgments

This work was supported by the collaborative participation in the Robotics Consortium sponsored by the U.S. Army Research Laboratory under the Collaborative Technology Alliance Program, Cooperative Agreement DAAD 19-01-2-0012. The U.S. Government is authorized to reproduce and distribute reprints for Government purposes not withstanding any copyright notation thereon.

References

1. W. Yu, O. Chuy, E. Collins and P. Hollis, *IEEE Transactions on Robotics* **26**, 340 (2010).
2. O. Chuy, E. Collins, W. Yu and C. Ordonez, Power modeling of a skid steered, wheeled robotic ground vehicle, in *Proceedings of the IEEE Conference on Robotics and Automation*, (Kobe, Japan, 2009).
3. U. Saranli, M. Buehler and D. Koditschek, *The International Journal of Robotics Research* **20**, 616 (2001).
4. J. Weingarten, G. Lopes, M. Buehler, R. Groff and D. Koditschek, Automated gait adaptation for legged robots, in *Proceedings of the IEEE Conference on Robotics and Automation*, (New Orleans, USA, 2004).
5. G. C. Haynes, J. Pusey, R. Knopf, A. M. Johnson and D. E. Koditschek, Laboratory on legs: An architecture for adjustable morphology with legged robots, in *SPIE Unmanned Systems Technology XIV (Conference 8387)*, 2012. To Appear.
6. K. C. Galloway, G. C. Haynes, B. D. Ilhan, A. M. Johnson, R. Knopf, G. Lynch, B. Plotnick, M. White and D. E. Koditschek, *X-RHex: A Highly Mobile Hexapedal Robot for Sensorimotor Tasks*, tech. rep., University of Pennsylvania (2010).
7. D. D. Dunlap, C. V. Caldwell, J. E. G. Collins and O. Chuy, *Motion Planning for Mobile Robots Via Sampling-Based Model Predictive Optimization*, *Recent Advances in Mobile Robotics* (InTech, 2011). <http://www.intechopen.com/books>.